Prepared for submission to JHEP HU-EP-18/18, HU-MATH 2018-05

Positivity of hexagon perturbation theory

Burkhard Eden,[a] **Yunfeng Jiang,**[b] **Marius de Leeuw,**[c] **Tim Meier,**[a] **Dennis le Plat,**[a] **Alessandro Sfondrini**[b]

[a] *Institut für Mathematik und Physik, Humboldt-Universität zu Berlin, Zum großen Windkanal 6, 12489 Berlin, Germany*

[b] *Institut für theoretische Physik, ETH Zürich, Wolfgang-Pauli-Straße 27, 8093 Zürich, Switzerland*

[c] *School of Mathematics & Hamilton Mathematics Institute Trinity College Dublin Dublin, Ireland*

E-mail: eden@math.hu-berlin.de, jiangyu@phys.ethz.ch, mdeleeuw@maths.tcd.ie, tmeier@physik.hu-berlin.de, diplat@physik.hu-berlin.de, sfondria@itp.phys.ethz.ch

Abstract: The hexagon-form-factor program was proposed as a way to compute three- and higher-point correlation functions in $\mathcal{N} = 4$ super-symmetric Yang-Mills theory and in the dual $AdS_5 \times S^5$ superstring theory, by exploiting the integrability of the theory in the 't Hooft limit. This approach is reminiscent of the asymptotic Bethe ansatz in that it applies to a large-volume expansion. Finite-volume corrections can be incorporated through Lüscher-like formulae, though the systematics of this expansion are largely unexplored so far. Strikingly, finite-volume corrections may feature negative powers of the 't Hooft coupling g in the small-g expansion, potentially leading to a breakdown of the formalism. In this work show that the finite-volume perturbation theory for the hexagon is compatible with the weak-coupling expansion for arbitrary n-point functions, and is positive on the nose.

Contents

1 Introduction

Computing correlation functions is one of the central problems in quantum field theory. For a generic interacting theory, it is impossible to calculate such observables non-perturbatively. Usually one needs to perform an expansion in certain parameters. A typical example is the small-coupling expansion around a free theory, which can be performed by well-established techniques such as Feynman diagrams. In some special theories, more powerful alternative techniques may exist—usually based on symmetries. In integrable quantum field theories, the form-factor bootstrap approach is such an alternative. While most integrable models appear in one or two dimensions, integrability sometimes manifest itself in higher dimensional theories too, for instance through dualities such as AdS/CFT [1–3]. One of the most prominent examples is the $\mathcal{N} = 4$ supersymmetric Yang-Mills theory (SYM), dual to type-IIB supestrings on $\mathrm{AdS}_5 \times \mathrm{S}^5$. In the planar limit [4], the integrability of the spectral problem for the two-dimensional theory on the string worldsheet carries over to $\mathcal{N} = 4$ SYM in the guise of an integrable spin chain [5], see *e.g.* refs. [6, 7] for reviews. Interestingly, it was recently realised that integrability might play a role for more general observables too. Indeed, a generalisation of the form factor approach to $\mathcal{N} = 4$ SYM has been proposed in ref. [8] in terms of hexagonal tessellations; in the following we refer to this construction as the *hexagon approach*. This was initially proposed as a way to compute

planar three-point functions involving non-protected operators. Soon after, it was realised that those techniques could be adapted to higher-point planar correlation functions [9, 10] and at least to some extent to non-planar observables [11, 12].[1]

The hexagon approach is reminiscent of the "asymptotic" Bethe ansatz for the $\mathcal{N} = 4$ SYM spin chain [16], or of the Bethe-Yang equations in two dimensional integrable QFTs: it is only exact up to exponentially-small corrections in the volume of the theory—the R-charge of the $\mathcal{N} = 4$ SYM operators under consideration. In the spectral problem, such finite-size corrections can be interpreted as due to virtual ("mirror") particles wrapping the worlsdheet [17], similar to the Lüscher effects of relativistic theories [18, 19]. In the hexagon program, they can similarly be described as mirror particles probing the finite-size structure of the hexagon tessellation. For three-point functions, the first few finite-volume corrections can be explicitly computed and matched with small-coupling perturbation theory [8, 20–22]. Furthermore, in that context only a finite number of finite-volume corrections needs to be computed at each given order of the 't Hooft coupling expansion [21]. The situation is less clear for higher-point functions. The results of the hexagon approach for four- [9, 10] and five-point [23] functions and for certain non-planar observables [11, 12] match with the lowest orders of perturbation theory; such integrability computations account for the first few finite-volume corrections. Still, it was not shown so far that more complicated finite-volume effects (involving more mirror particles) can indeed be neglected at those orders. More generally, we do not know which finite-volume effects (*i.e.* how many mirror particles) we need to take into account at a given order of the 't Hooft-coupling expansion. Establishing this relation for general correlation functions is the aim of this paper.

The reason why this is a subtle problem—compared for instance to Lüscher corrections in the spectral problem—is that in the hexagon formalism mirror particle come in *three* distinct families. Indeed three of the six edges of the hexagon correspond to physical excitations, and the remaining three correspond to mirror (or anti-mirror) ones, leading to distinct kinematic regions. In the hexagon form factor, while physical processes yield non-negative powers of the 't Hooft coupling g^2 in the $g \ll 1$ expansion, mirror-anti-mirror processes yield a factor of g^{-2}. Naïvely, populating an hexagon with sufficiently many mirror magnons can make it so that a process which is extremely suppressed in "large-volume" appears *even at tree level* g^0. Even worse, in principle we might expect contributions to processes *with arbitrarily negative powers of* g^2*!*

Clearly such a situation would be disastrous for the hexagon program. Since several explicit computations match field theory results [9–12, 23], there should be a way to resolve this apparent issue. One possibility is that such multi-mirror-magnon processes indeed appear, but somehow cancel at appropriate orders in g^2 for correlation functions of physical states; this would make the formalism consistent in principle, but it would also make it almost impossible to extract physical data from the hexagon construction for generic observables without knowing *a priori* which processes cancel and which do not. The other much more appealing possibility is that there exist a refined estimate where, as we add more and more mirror magnons, we obtain higher and higher terms in the g^2 expansion. In this paper we show that this is the case *for arbitrary (planar and non-planar) correlation functions* of protected operators, obtaining an explicit formula relating the number of

[1] Non-planar observables in $\mathcal{N} = 4$ SYM are also being actively investigated by other integrability-based approaches, see *e.g.* refs. [13, 14], as well as ref. [15] for a review of earlier developments.

mirror magnons to the order in the small-g expansion. We call this property the *positivity* of the hexagon perturbation theory. This also extends to the case of non-protected operators, which however depends more subtly on which particular correlator we consider.

The paper is structured as follows: we start by reviewing some essential features of the hexagon approach in section 2. In section 3 we present our main result: an improved estimate for the contribution of mirror processes to the g-expansion, which is *bounded from below*, valid for any correlator of BPS operators; we also comment on the extension to non-BPS operators. In section 4 we apply these ideas to the computation of planar four-point functions of BPS operators. We conclude in section 5. We also present an alternative (algorithmic) derivation of our improved bound in appendix A.

2 Review of hexagon form factors

When computing four- and higher-correlation functions we need to triangulate a punctured Riemann surface (the sphere, for planar correlators). The edges of such triangles are the "mirror" edges of the hexagons. By blowing up the punctures to small circles we can add three more "physical" edges corresponding to arcs on those circles. Since we are interested in obtaining an estimate valid *for any correlation functions*, below we shall not make any assumption on how hexagons are glued together. Instead, we will consider a single hexagon.

2.1 Form factor for a single hexagon

As we mentioned, the key idea of the hexagon approach to correlation functions is to decompose any correlation function into a hexagonal tessellation. To "glue" together such a tessellation it is necessary to insert a complete basis of states for each of the three "mirror" edges. This amounts to populating the hexagon with mirror magnons. Notice that, precisely because mirror magnons arise from "gluing", they are shared by two contiguous hexagons. Taking this into account, the hexagon form factor with $\mathbf{u}, \mathbf{v}, \mathbf{w}$ sets of mirror magnons and $\mathbf{x}, \mathbf{y}, \mathbf{z}$ sets of physical magnons takes the form

$$\text{hexagon} \sim \sqrt{\mu_{\mathbf{u}}\mu_{\mathbf{v}}\mu_{\mathbf{w}}}\, e^{\frac{i}{2}\tilde{E}_{\mathbf{u}}\ell_{\mathbf{u}}+\cdots}\, e^{i\psi\mathbf{J}+\cdots}\, \langle\, \mathfrak{h} \,|\, \mathbf{z}^{4\gamma}, \mathbf{u}^{3\gamma}, \mathbf{y}^{2\gamma}, \mathbf{v}^{\gamma}, \mathbf{x}^{0\gamma}, \mathbf{w}^{-\gamma} \,\rangle\,. \tag{2.1}$$

Some comments are in order. Here μ is the mirror measure corresponding to each mirror magnon; we only assign "half" of such a measure to each hexagon, as mirror magnons are shared across two hexagons. For the same reason, we split in half the "bridge length" ℓ along which each magnons propagates. Next, we allow for an arbitrary chemical potential ψ (for any possible magnon charge) which is needed to describe four- and higher-point functions [9, 10]. The powers of γ identify how many time we perform the mirror transformation in the notation of ref. [21]. Notice that physical particles sit at even-γ edges, and mirror ones at odd-γ ones. Finally,[2] the hexagon form factor $\mathfrak{h}$ can then be related to the centrally extended $\mathfrak{su}(2|2)$ (bound state) S-matrix S_{ij} [24, 25]

$$\langle\, \mathfrak{h} \,|\, \mathbf{z}^{4\gamma}, \mathbf{u}^{3\gamma}, \mathbf{y}^{2\gamma}, \mathbf{v}^{\gamma}, \mathbf{x}^{0\gamma}, \mathbf{w}^{-\gamma} \,\rangle \sim \prod_{i<j} h_{ij} S_{ij}\,, \tag{2.2}$$

[2] In order to compute a complete correlation function it would be necessary to consider all hexagons in the tessellation, sum over partitions for physical excitations, sum over all possible mirror particles and integrate over their rapidities—and normalise the result appropriately. The detail of this, as we mentioned, depend on the particular correlator we are computing; here we will not perform this procedure, as we aim at an estimate as general as possible.

up to a suitable projection in flavour space on the right-hand side [8]. The hexagon factor h_{ij} for two bound states with bound state numbers Q_1, Q_2 is given by

$$h_{12} = \prod_{k=-\frac{Q_1-1}{2}}^{\frac{Q_1-1}{2}} \prod_{l=-\frac{Q_2-1}{2}}^{\frac{Q_2-1}{2}} h(u_1^{[2k]}, u_2^{[2l]})\,, \tag{2.3}$$

$$h(u_1,u_2) = \frac{x_1^- - x_2^-}{x_1^- - x_2^+} \frac{1-\frac{1}{x_1^- x_2^+}}{1-\frac{1}{x_1^+ x_2^+}} \frac{1}{\sigma(u_1,u_2)}\,. \tag{2.4}$$

The dressing factor σ_{12} is given by the BES phase [26]. The purpose of this paper is to explore whether a perturbative weak-coupling expansion is compatible with the hexagon approach. In order to address we need to understand the weak-coupling expansion of

$$\mathcal{S}_{ij} = h_{ij} S_{ij}\,, \tag{2.5}$$

i.e. of the $su(2|2)$ S matrix dressed by the hexagon scalar factor, in different kinematic channels.

2.2 Weak-coupling expansions

In order to see how different pieces of eq. (2.1) scale when $g \ll 1$, let us collect here the weak-coupling expansion of the relevant quantities, and fix our conventions.

Conventions, We need to compute the S-matrix between magnons with different mirror orientations. For consistency, we will work with the *string-frame* S matrix [27], see also ref. [6] for a review. We follow the conventions of [8, 23], where the bound-state S matrix S is normalized such that the scattering of the highest-weight fermionic state is set to unity. Moreover, we note that the dressing factor σ for two bound states with bound-state numbers $Q_{1,2}$ satisfies the following crossing equations [28]

$$\sigma_{12}(u_1^{2^\gamma}, u_2) = \left(\frac{x_2^-}{x_2^+}\right)^{Q_1} \frac{x_1^- - x_2^+}{x_1^- - x_2^-} \frac{1-\frac{1}{x_1^+ x_2^+}}{1-\frac{1}{x_1^+ x_2^-}} \prod_{k=1}^{Q_1-1} \frac{u_1 - u_2 - i\frac{Q_2-Q_1+2k}{g}}{u_1 - u_2 + i\frac{Q_2-Q_1+2k}{g}} \frac{1}{\sigma_{12}(u_1,u_2)}, \tag{2.6}$$

$$\sigma_{12}(u_1, u_2^{-2^\gamma}) = \left(\frac{x_1^+}{x_1^-}\right)^{Q_2} \frac{x_1^- - x_2^+}{x_1^- - x_2^-} \frac{1-\frac{1}{x_1^+ x_2^+}}{1-\frac{1}{x_1^+ x_2^-}} \prod_{k=1}^{Q_1-1} \frac{u_1 - u_2 - i\frac{Q_2-Q_1+2k}{g}}{u_1 - u_2 + i\frac{Q_2-Q_1+2k}{g}} \frac{1}{\sigma_{12}(u_1,u_2)}. \tag{2.7}$$

The dressing factor respects unitarity so that $\sigma_{12} = 1/\sigma_{21}$. By using the crossing equations and unitarity we can, for instance, relate all the dressing phases between mirror and anti-mirror particles to $\sigma(u^\gamma, v^\gamma)$.

Expansions. Let us spell out the expansions of the different scattering matrices $\mathcal{S}$ for small coupling g. These can be straightforwardly checked for the scattering of fundamental magnons and, by the fusion procedure, the results carry over to bound-state S matrices.[3] For virtual particles with the same mirror orientation, we find that the expansion starts at order g^2

$$\mathcal{S}(u_i^{3^\gamma}, u_j^{3^\gamma}) \sim \mathcal{S}(u_i^\gamma, u_j^\gamma) \sim \mathcal{S}(u_i^{-^\gamma}, u_j^{-^\gamma}) \sim g^2. \tag{2.8}$$

[3] We have explicitly checked all these expansions for the $Q = 2$ bound-state S matrix.

For physical particles, we find that the expansion always starts at order 1

$$\mathcal{S}(u_i, u_j) \sim \mathcal{S}(u_i^{2\gamma}, u_j^{2\gamma}) \sim \mathcal{S}(u_i^{4\gamma}, u_j^{4\gamma}) \sim g^0 \tag{2.9}$$

$$\mathcal{S}(u_i^{2\gamma}, u_j) \sim \mathcal{S}(u_i^{4\gamma}, u_j) \sim \mathcal{S}(u_i^{4\gamma}, u_j^{2\gamma}) \sim g^0. \tag{2.10}$$

Next we expand the S matrix for the scattering processes that involve virtual magnons from different edges

$$\mathcal{S}(u_i^{3\gamma}, v_j^{\gamma}) \sim \mathcal{S}(u_i^{3\gamma}, u_j^{-\gamma}) \sim \mathcal{S}(u_i^{\gamma}, u_j^{-\gamma}) \sim g^{-2}. \tag{2.11}$$

This is the contribution that makes it possible, at least in a naïve estimate, to obtain arbitrarily negative powers of g^2 when adding mirror magnons. Finally, let us also consider the scattering between a virtual and a physical magnon. The dressed S matrix is of order 1 unless the virtual magnon is on the edges that are connected to the physical magnon

$$\mathcal{S}(u_i^{n\gamma}, u_j^{(n+3)\gamma}) \sim \begin{cases} g^{-1} & \text{if magnon 1 is boson } \phi^a, \\ g^0 & \text{if magnon 1 is fermion } \psi^\alpha, \end{cases} \tag{2.12}$$

where $n = 0, 2, 4$. In the last two expansions we encounter yet another potential problem, as the negative powers of the coupling constant g can potentially lead to arbitrary negative powers of the coupling constant in the hexagon expansion.

Multiple scattering. A remarkable observation which will be crucial in what follows is that the weak-coupling expansion of the scattering process between three virtual magnons may scale "better than naïvely expected". Specifically, let us take three mirror magnons from three different edges. We then find

$$\mathcal{S}_{12}(u_i^{3\gamma}, v_j^{+\gamma})\, \mathcal{S}_{13}(u_i^{3\gamma}, w_j^{-\gamma})\, \mathcal{S}_{23}(v_i^{+\gamma}, w_j^{-\gamma}) \;\sim\; g^{-2}. \tag{2.13}$$

We would expect this process to scale like g^{-6}, but it turns out that the most divergent contributions cancel out, so that the process scales *four orders higher* in the g expansion than we would expect! This is a rather striking and unique property of the S matrix: we have verified that, up to scattering six magnons, there are no further identities of this type in any mirror channel. Finally, it is also interesting to note that a similar (weaker) triple-scattering property arises also in the case where one of the magnons is physical, one virtual magnon is adjacent and the other virtual magnon is across the physical magnon,

$$\begin{aligned} \mathcal{S}_{12}(u_i^{3\gamma}, v_j^{+\gamma})\, \mathcal{S}_{13}(u_i^{3\gamma}, x_j^{0\gamma})\, \mathcal{S}_{23}(v_i^{+\gamma}, x_j^{0\gamma}) \;&\sim\; g^{-2}, \\ \mathcal{S}_{12}(u_i^{3\gamma}, w_j^{-\gamma})\, \mathcal{S}_{13}(u_i^{3\gamma}, x_j^{0\gamma})\, \mathcal{S}_{23}(x_j^{0\gamma}, w_i^{-\gamma}) \;&\sim\; g^{-2}. \end{aligned} \tag{2.14}$$

According to (2.12) this could have been of order g^{-3} when the physical magnon is a boson. What is more, the above relation can be generalized to an arbitrary number of physical magnons:

$$\begin{aligned} \mathcal{S}_{12}(u_i^{3\gamma}, v_j^{+\gamma}) \prod_j \mathcal{S}_{1j}(u_i^{3\gamma}, x_j^{0\gamma})\, \mathcal{S}_{2j}(v_i^{+\gamma}, x_j^{0\gamma}) \;&\sim\; g^{-2}, \\ \mathcal{S}_{12}(u_i^{3\gamma}, w_j^{-\gamma}) \prod_j \mathcal{S}_{1j}(u_i^{3\gamma}, x_j^{0\gamma})\, \mathcal{S}_{2j}(x_j^{0\gamma}, w_i^{-\gamma}) \;&\sim\; g^{-2}. \end{aligned} \tag{2.15}$$

3 Positivity of hexagon perturbation theory

Let us now derive an explicit formula for the order in $g \ll 1$ at which a given hexagon configuration starts to contribute to the perturbative expansion. We first consider the case where we have only mirror excitations on the three mirror edges; this is the relevant case when computing arbitrary correlation functions of half-BPS operators.

3.1 Naïve estimate of of 't Hooft-coupling order

The contribution of a single hexagon (2.1) is a little simpler for BPS operators

$$\sqrt{\mu_{\mathbf{u}}\mu_{\mathbf{v}}\mu_{\mathbf{w}}}\, e^{\frac{i}{2}\tilde{E}_{\mathbf{u}}\ell_{\mathbf{u}}+\dots}\, e^{i\psi\mathbf{J}+\dots}\, \langle\, \mathfrak{h}\,|\varnothing, \mathbf{u}^{3\gamma}, \varnothing, \mathbf{v}^{\gamma}, \varnothing, \mathbf{w}^{-\gamma}\rangle = O(g^p)\,. \tag{3.1}$$

This scales like g^p when $g \ll 1$, where the order p is, naïvely

$$p_{\text{naïve}} = \sum_{i=1}^{3} N_i(1+\ell_i) + 2\sum_{i=1}^{3}\frac{N_i(N_i-1)}{2} - 2N_1N_2 - 2N_1N_3 - 2N_2N_3\,, \tag{3.2}$$

where we have introduced the short-hand notations

$$|\mathbf{u}| = N_1, \qquad |\mathbf{v}| = N_2, \qquad |\mathbf{w}| = N_3. \tag{3.3}$$

Let us see how the different terms arise. Firstly, the first term in eq. (3.2) is given the the contribution of "half the measure" which scales as g^1 for each mirror magnon, plus half of the contribution of the bridge lengths. Next, when scattering all particles on the ith mirror edge among themselves, we have a total of $N_i(N_i-1)/2$ processes, each contributing g^2. Finally, and *herein lies the rub*, when scattering magnons from different edges we get *negative* contributions, of order g^{-2} for each scattering event. We can rewrite the naïve estimate (3.2) as

$$\begin{aligned} p_{\text{naïve}} &= \sum_{i=1}^{3} N_i\ell_i + \sum_{i=1}^{3} N_i^2 - 2N_1N_2 - 2N_1N_3 - 2N_2N_3 \\ &= \sum_{i=1}^{3} N_i\ell_i + (N_1-N_2)^2 + N_3^2 - 2N_3(N_1+N_2)\,, \end{aligned} \tag{3.4}$$

which is clearly *unbounded from below*, for instance when $N_1 \sim N_2 \gg N_3 \gg \ell_i$.

Improving the estimate. Bearing in mind the observation of eq. (2.13), we can get a better estimate for the scaling of a single hexagon, namely

$$p = p_{\text{naïve}} + 4T(N_1, N_2, N_3)\,, \tag{3.5}$$

where $T(N_1, N_2, N_3)$ is the number of "triple" scattering events such as the ones of eq. (2.13). We are therefore interested in arranging the scattering in such a way as to maximise such triple scattering processes.

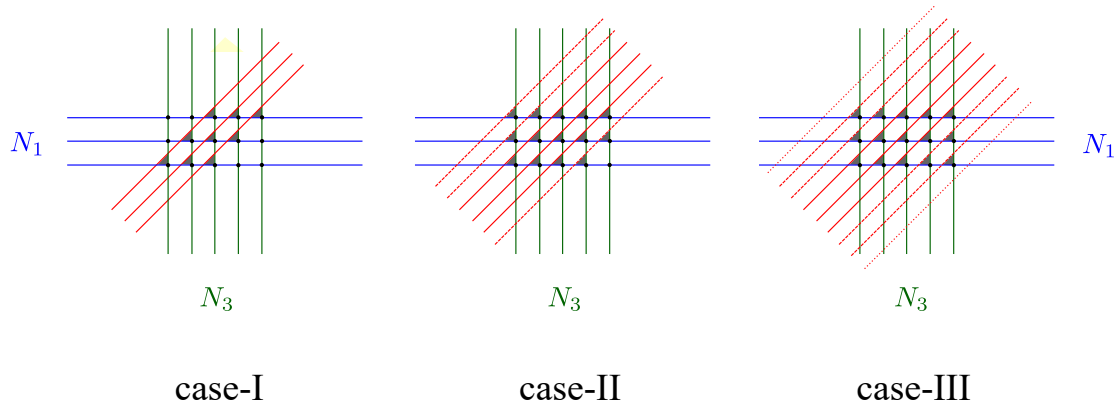

Figure 1. Diagrammatic representation of scattering processes involving three sets of mirror magnons labelled by N_1, N_2 and N_3, corresponding to particles of type **u**, **v** and **w**, respectively. We start by drawing the lines corresponding to N_1 and N_3 (assuming for definiteness $N_1 \leq N_3$) and then place, one by one, the diagonal lines corresponding to N_2 in such a way as to maximise the triple scattering of eq. (2.13)—the dark triangles. As detailed in the main text, we see three distinct behaviours depending on how many diagonal lines we need to place: for the first few, which we place in the purple region (see left panel), we get a constant number of triangles per diagonal line. After a certain point (yellow region, middle panel), the number of triangles decreases as we add lines. Eventually, adding more diagonal lines does not yield any new triangle (right panel).

3.2 Triple scattering processes

It is convenient to introduce a diagrammatic representation of the scattering processes which we will consider. In practice, we have three sets of lines $\{\mathbf{u}\}$, $\{\mathbf{v}\}$, $\{\mathbf{w}\}$, which we want to rearrange by reversing their order,

$$(u_1, \dots u_{N_1}, v_1, \dots v_{N_2}, w_1, \dots w_{N_3}) \to (w_{N_3}, \dots w_1, v_{N_2}, \dots v_1, u_{N_1}, \dots u_1). \tag{3.6}$$

For the purpose of counting the triple-intersection of lines of type u, v and w the rearrangement within each set $\{\mathbf{u}\}$, $\{\mathbf{v}\}$, $\{\mathbf{w}\}$ is irrelevant. Hence we can consider the slightly simpler process

$$(u_1, \dots u_{N_1}, v_1, \dots v_{N_2}, w_1, \dots w_{N_3}) \to (w_1, \dots w_{N_3}, v_1, \dots v_{N_2}, u_1, \dots u_{N_1}). \tag{3.7}$$

We have represented such a scattering process in figure 1. We start by drawing N_1 horizontal and N_3 vertical lines, which we can do unambiguously. For definiteness, we shall assume

$$N_1 \leq N_3\,. \tag{3.8}$$

Next, we can add one by one the N_2 lines corresponding to **v**, which should go from south-west to north-east of the figure. This can be done in several equivalent ways, owing to the Yang-Baxter equation. We want to do so in such a way as to maximise the triple scattering discussed above, which here results in a triangular vertex (see also the figure). It is convenient to distinguish three cases, depending on the value of N_2.

Case I. Looking at the leftmost panel in figure 1, we imagine to add a single diagonal line. Clearly we get at most as many triangles as we have horizontal lines, *i.e.* N_1 triangles—recall that $N_1 \leq N_3$. We can go on adding diagonal lines as long as we saturate the purple

area in the region; indeed we can do so $N_3 - N_2 + 1$ times at most. Therefore, we have that

$$T(N_1, N_2, N_3) = N_2\, N_1, \qquad N_2 \leq N_3 - N_1 + 1\,. \tag{3.9}$$

Case II. Let us keep adding diagonal lines, looking this time at the middle panel of figure 1. To maximise the number of triangles, we add diagonal lines just above or just below those we had drawn above. We have two choices with $(N_1 - 1)$ triangles (above and below), two choices with $(N_1 - 2)$ triangles, and so on. Adding one line at the time, we get the sequence

$$N_1 - 1, N_1 - 1, N_1 - 2, N_1 - 2, N_1 - 3, N_1 - 3, \dots\,, \tag{3.10}$$

which reaches zero in $2N_1$ steps. Therefore, as long as $N_2 \leq N_3 - N_1 + 1 + 2N_1 = N_3 + N_1 + 1$, the number of new triangles (in the yellow region of the figure) is given by the sum

$$\sum_{j=1}^{K} \Big[N_1 - \frac{(2j + 1 - (-1)^j)}{4} \Big], \tag{3.11}$$

which can run up at most $K = N_2 - (N_3 - N_1 + 1)$ steps. The slightly odd summand just reproduces the sequence (3.10). Bearing in mind that we have $N_1(N_3 - N_1 + 1)$ triangles in the purple region, with a little algebra we find that the total number of triangles is at most

$$T(N_1, N_2, N_3) = \frac{N_1 N_2 + N_1 N_3 + N_1 N_2}{2} - \sum_{i=1}^{3} \frac{N_i^2}{4} + \frac{1 + (-1)^{\sum_i N_i}}{8}, \qquad \text{for} \quad N_3 - N_1 + 1 < N_2 \leq N_3 + N_1 + 1\,. \tag{3.12}$$

We shall comment later on the fractional coefficients; for the moment, suffice it to say that by construction this number is an integer, albeit an odd-looking one.

Case III. Finally, we can keep adding diagonal lines like in the rightmost panel of figure 1. This does not generate any new triangles. Therefore, we can just use the previous estimate, taking the limit of the sum (3.11) to be the maximal allowed value $M = 2N_1$. Then we get that

$$T(N_1, N_2, N_3) = N_3\, N_1, \quad N_3 + N_1 + 1 < N_2\,, \tag{3.13}$$

as we could have expected from the graphical representation: we simply have on triangle for each vertex between horizontal and vertical lines.

3.3 Improved estimate of 't Hooft-coupling order

Armed with these estimates, it is not difficult to see case by case at which order $O(g^p)$ a digram with (N_1, N_2, N_3) mirror particles contributes.

Case I. Here we have

$$p = \sum_{i=1}^{3} N_i \ell_i + (N_3 - N_1 - N_2)^2, \qquad N_2 \leq N_3 - N_1 + 1\,, \tag{3.14}$$

which is positive semi-definite regardless of the values of ℓ_i.

Case II. In the second case we are left with

$$p = \sum_{i=1}^{3} N_i \ell_i + \frac{1 + (-1)^{\sum_i N_i}}{2}, \qquad N_3 - N_1 + 1 < N_2 \leq N_3 + N_1 + 1\,. \tag{3.15}$$

Note that the fact that p is not necessarily even is due to the fact that we are considering *a single* hexagon, and have split the measure and bridge length as in eq. (2.1). At weak coupling, we expect the expansion to be in powers of g^2 when all hexagons are glued together.

Case III. Similarly to case I we have

$$p = \sum_{i=1}^{3} N_i \ell_i + (N_2 - N_1 - N_3)^2, \qquad N_2 > N_3 + N_1 + 1\,. \tag{3.16}$$

Infinite chains of mirror magnons. Notice that while the present estimate makes p bounded from below, unlike the orginal naïve estimate (3.2), it is still possible to have infinitely many processes contributing at a given order. This can be achieved by setting *e.g.* N_3 to a fixed values and varying N_1 and N_2, *provided that both bridge lengths* ℓ_1, ℓ_2 *vanish*. More generally, it is only possible for infinitely many magnons to contribute at a given order of the small-coupling expansion when two bridge lengths vanish. This situation may well appear when computing correlators, and is all the more frequent considering non-planar topologies, see *e.g.* ref. [11]. We could not find a way to rule out such processes on general grounds, though it is possible to make some progress when considering particular correlators. In section 4 we will look in detail at how these processes appear in the four-point functions of BPS operators. We will see that it is still possible to use the bound we have obtained here, along with some observations from field theory, to reduce the computation to a *finite* set of mirror exchanges.

3.4 Physical magnons

From eq. (2.12) we see that, as long as physical magnons are given by fundamental *fermionic* excitations—for instance, for non-BPS operators in the $sl(2)$ sector—our estimates from the previous section apply immediately since no negative powers of g emerge from physical-mirror scattering. Things are a little more involved if we allow for bosonic excitations. Consider for instance an hexagon containing a set of physical particles $\{\mathbf{x}\}$ in the $so(6)$ sector, so that the hexagon is schematically

$$\sqrt{\mu_{\mathbf{u}}\mu_{\mathbf{v}}\mu_{\mathbf{w}}}\, e^{\frac{i}{2}\tilde{E}_{\mathbf{u}}\ell_{\mathbf{u}}+\cdots}\, e^{i\psi\mathbf{J}+\cdots}\, \langle\, \mathfrak{h}\,|\varnothing, \mathbf{u}^{3\gamma}, \varnothing, \mathbf{v}^{\gamma}, \mathbf{x}, \mathbf{w}^{-\gamma}\rangle = O(g^p)\,. \tag{3.17}$$

The contribution of the $M = |\mathbf{x}|$ physical $so(6)$ magnons naïvely would be

$$p \to p - M\, N_2 \qquad \text{naïvely}, \tag{3.18}$$

which once again would yield an estimate which is unbounded from below as N_2 grows. Again we can improve our estimate, this time using the triangle identity (2.15).

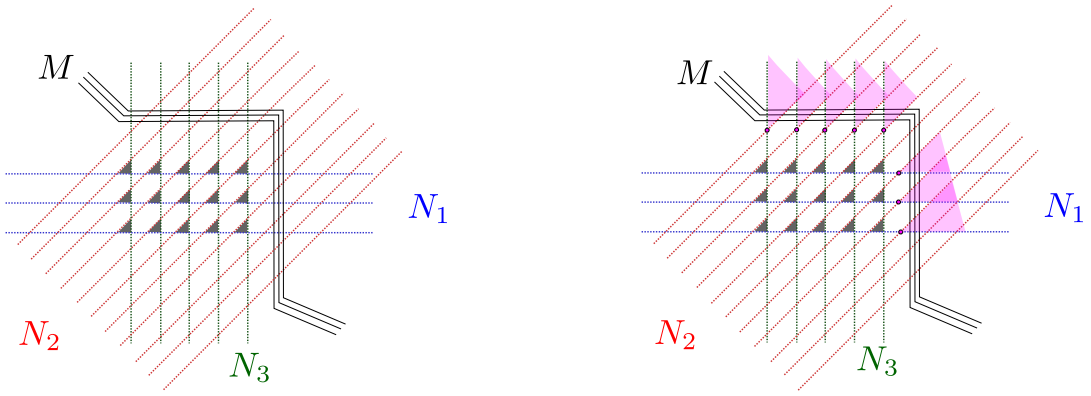

Figure 2. We draw again the scattering processes of figure 1, focussing on case III and adding M physical magnons. To guide the eye, we have dotted the lines corresponding to mirror magnons. On the left, we have $M\,N_2$ scattering events between physical magnons and magnons on the opposing edge. On the right panel, we highlight the "cones" emanating from the scattering of a mirror particle on the opposite edge with one from the adjacent edge; this is the vertex of the cone, and it is marked by a dot. There are clearly $N_1 + N_3$ such cones.

Improved estimate. Consider the picture in figure 2. Here we have further decorated a graph such as the one of figure 1 by adding a new set of lines, denoted by M, and corresponding to M physical magnons. We are focussing here on what we called case III in figure 1, which happens when

$$N_2 > N_1 + N_3 + 1\,. \tag{3.19}$$

The reason is that the only runaway behaviour can arise as $N_2 \to \infty$, which constrains us to this scenario. We have already already maximised the number of u-v-w triangles following the logic explained above. Now we want to maximise the number of multiple scattering events as in eq. (2.15). These can be thought of as "cones" emanating either from an u-v triangles or v-w vertex, and involving an arbitrary number of physical particles x. From the figure we see that there are N_1 u-v vertices and N_3 v-w vertices, bearing (3.19) in mind, for a total of $N_1 + N_3$ cones. Furthermore, each cone contains M scattering events between physical magnons and mirror magnons on the opposite edge. Hence, our naïve estimate is improved by a factor of $M(N_1 + N_3)$. All in all,

$$p \to p - M\,(N_2 - N_1 - N_3)\,, \tag{3.20}$$

so that in presence of M physical magnons

$$p = \sum_{i=1}^{3} N_i \ell_i + (N_2 - N_1 - N_3)(N_2 - N_1 - N_3 - M)\,. \tag{3.21}$$

Hence p is still bounded from below, even if its minimum value (as N_2 varies) can become negative. In particular, we find that

$$p_{\rm min} = N_1(\ell_1 + \ell_2) + N_3(\ell_3 + \ell_2) - \frac{M^2 - 2M}{4}\,, \tag{3.22}$$

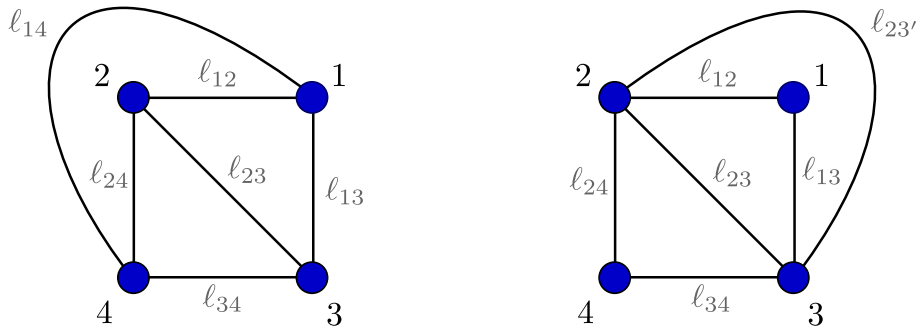

Figure 3. Hexagon tessellations for planar four-point functions. The four points lie on a sphere which we represent on the plane. Solid lines represent strands of propagators, see eq. (4.3), which dictate in which way to tessellate the diagram. Up to relabeling the points 1234 these are the only planar tree-level diagrams [9, 10]. Planarity restricts the ℓ_{ij} that can be non-zero to those in the figure. Still, it is possible that a subset of the solid lines in the figure have $\ell_{ij} = 0$, as we shall see below.

which is bounded from below for fixed M (*i.e.*, for any given physical state).[4] Similar bounds can be derived for more general configurations of physical magnons.

Application to physical correlators of non-BPS operators. Our estimate for p remains bounded from below and is only slightly worsened by the inclusion of physical magnons if those sit in the $so(6)$ sector. Moreover, we might expect the estimate to further improve when restricting to a particular topology for the correlator—as it is the case for three-point function [21]. This could arise both from glueing different hexagons, from summing over the partitions of physical magnons, and from exploiting the fact that physical states satisfy the Bethe ansatz equations. It is still a bit surprising that $so(6)$ physical excitations behave so differently from other magnons in the physical-mirror scattering. This is essentially due to "string-frame" factors [6, 27] in the $su(2|2)$ scattering matrix, which in the mirror kinematics affects the g-scaling. Historically, the hexagon formalism has been formulated in a hybrid of the spin-chain and string frames [8], where for instance crossing transformations are performed in the string frame, but edge-widths are written in terms of spin-chain lengths; it is also apparently necessary to explicitly keep track of frame factors in certain computations [10, 23]. As those computations have so far focussed on non-protected operators in the $sl(2)$ sector only, it would be very interesting to derive correlation functions of operators from the $su(2)$ subsector via the hexagon approach, and understand how these match the field-theory results.

4 Application to planar BPS four-point functions

In this section we apply our results above to the computation of a particular correlation function; we will especially focus on the issue of infinite chains of mirror magnons. Let us consider a planar four-point function of half-BPS operators

$$\langle\, \mathcal{O}_{k_1}(x_1)\, \mathcal{O}_{k_2}(x_2)\, \mathcal{O}_{k_3}(x_3)\, \mathcal{O}_{k_4}(x_4)\,\rangle\,, \qquad \mathcal{O}_k \,=\, \mathrm{Tr}(\hat{Z}^k)\,, \tag{4.1}$$

[4] It is also worth noticing that the length L of a physical operator containing M $so(6)$ excitations is $L \geq M$. This means that, for the adjacent mirror edges, $\ell_1 + \ell_3 \geq M$, which further improves our estimate.

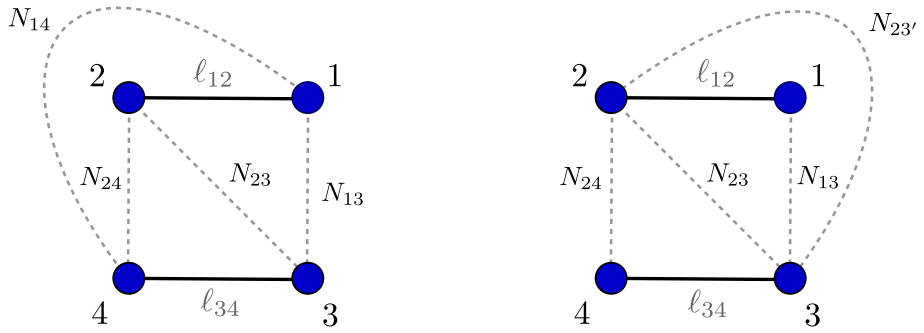

Figure 4. Four-point functions with four vanishing bridge lengths. The resulting hexagon tessellations allow for infinite chains of mirror magnons (along the zero-length bridges) already at order g^0.

where the six real scalars ϕ^I of $\mathcal{N}=4$ SYM are rewritten in the linear combination $\hat{Z}=\sum_{I=1}^{6}\phi^I Y^I$, with Y a complex null vector. Two fields $\hat{Z}_i(x_i)$ and $\hat{Z}_j(x_j)$ have the free propagator

$$\Pi_{ij}=\frac{Y_i\cdot Y_j}{|x_i-x_j|^2}\,. \tag{4.2}$$

As proposed in refs. [9, 10], to compute such a four-point function by hexagon tessellations we start by listing all propagator combinations with the right conformal weights k_1,k_2,k_3,k_4. These are simply

$$\left\{\Pi_{12}^{\ell_{12}}\,\Pi_{13}^{\ell_{13}}\,\Pi_{14}^{\ell_{14}}\,\Pi_{23}^{\ell_{23}}\,\Pi_{24}^{\ell_{24}}\,\Pi_{34}^{\ell_{34}}\;:\quad k_i=\sum_j \ell_{ij}\right\}. \tag{4.3}$$

Notice that the number of propagator ℓ_{ij} in the strand going from point i to point j is exactly the *bridge length* which we discussed in section 3, and which is a crucial part of our final estimate for p, see eq. (3.5) and below. We are interested in planar graphs, *i.e.* graphs that can be drawn on a sphere without intersecting the propagators; not all assignments of ℓ_{ij} give rise to such graphs. It is easy to see this diagrammatically. In figure 3 we show the choices of ℓ_{ij} that give rise to planar graphs and the relative hexagon tessellation. For any allowed choice of propagators resulting in such a planar topology from the set (4.3), we have to decorate the figure with all mirror magnons allowed by our estimates of section 3, up to the order in g^2 in which we are interested.

Notice that already at the lowest orders in $g\ll 1$ this can involve an *infinite chain of mirror particles*. More specifically, this can happen when sufficiently many mirror edges have vanishing bridge length. Consider figure 4, and notice that *e.g.* in the left diagram

$$\ell_{24}=\ell_{23}=\ell_{13}=\ell_{14}=0\,. \tag{4.4}$$

Let us now estimate the order g^p at which this graph contriutes, restricting to the case where there are no mirror magnons on the non-zero length bridges ($N_{12}=N_{34}=0$), which turns out to be the key example. Then we have[5]

$$\begin{aligned} p=&\;2\,(N_{24}^2+N_{23}^2+N_{13}^2+N_{14}^2-N_{24}N_{23}-N_{23}N_{13}-N_{13}N_{14}-N_{12}N_{24})\\ =&\;(N_{24}-N_{23})^2+(N_{23}-N_{13})^2+(N_{13}-N_{14})^2+(N_{14}-N_{24})^2\,. \end{aligned} \tag{4.5}$$

[5]Notice that here there is no possibility to have "triple scattering events" (see section 3) and our estimate for the 't-Hooft coupling order g^p coincides with the naïve one (3.2).

In the first line, the quadratic contributions come from the interaction of magnons on the same mirror edge (including the mirror measure), while the bilinear terms come from scattering magnons on different edges within the same hexagon. The expression on the second line makes it transparent that we can have infinitely many mirror magnons contributing at given orders of perturbation theory g^p by tuning the values of N_{ij}. For instance, this happens when $N_{24} = N_{23} = N_{13} = N_{14} = N$ and we let $N = 1, 2, \ldots$. This process should contribute *already at tree-level!* Going to slightly higher orders in g^2, more trouble appears. Take for instance $N = N_{24} = N_{23} = N_{13} = N_{14} - 1$: all these processes would appear at order g^2; similarly, we find more such "chains" at higher orders. Moreover, depending on the loop order which interests us we may also need to consider more complicated processes. For instance, by putting a single mirror magnon on edge 12 ($N_{12} = 1$) we obtain

$$p = 2\ell_{12} + (N_{24} - N_{23})^2 + (N_{23} - N_{13} + 1)^2 + (N_{13} - N_{14})^2 + (N_{14} - N_{24} + 1)^2, \quad (4.6)$$

where it was crucial to use the improved estimate of section 3 for p to be positive. We see that such processes give infinite chains of magnons starting from order $g^{2\ell_{12}}$. Clearly the same can be done on edge 34.

What is the physical interpretation of these processes? Since they only stem from disconnected tree-level graphs, they seem quite pathological; however, it is not obvious that we can discard them. The tree-level graph should indeed be trivial, so that the g^0 contribution from this infinite chain of magnons vanish. However, at higher orders, we might imagine that introducing mirror particles corresponds to inserting virtual gluon lines in field theory [11], which might give a connected four-point graph. At one loop, it has been shown that the hexagon prediction *without any infinite chain* matches the field theory result [10], so it seems that these vanish at that order too. What about higher loops?

As such infinite chains can hardly be evaluated directly, to address this problem it is useful to notice that there is some redundancy in the hexagon formulation, which results in linear identities among apparently unrelated mirror-magnon processes. In particular, we note the following conditions

1. When several ℓ_{ij}s vanish it is possible to embed the same tree-level graph into different tessellations. It is natural to assume that all such embeddings are equivalent. This condition, which we call *embedding invariance*, has been checked on several examples so far [9–11].

2. The hexagon formula (3.1) depends only on the lengths of the bridges which contain at least one mirror magnon [10]; hence diagrams with no magnons on edge ij give identical integrals for any ℓ_{ij}. We call this property *forgetfulness* of the hexagons.

3. In $\mathcal{N} = 4$ SYM there exist *magic identities* for four point functions [29], due to superconformal symmetry.

4. It is also known that certain four-point functions obey *non-renormalisation* theorems [30–32]; this happens for of "extremal" and "sub-extremal" correlators, in which the lengths of the four operators obey $L_1 = L_2 + L_3 + L_4$ and $L_1 = L_2 + L_3 + L_4 - 2$, respectively.

5. Furthermore, we can match correlators *explicit results* [33] for the $SU(N)$ gauge group; this gives constrains for the mirror-magnon processes that appear in more general diagrams too.

Using these criteria, we see[6] that infinite chains of mirror magnons of the type of eq. (4.6) *vanish* also at order g^4 (we might have expected such processes to appear when $\ell_{12} = 2$ or $\ell_{34} = 2$). As for the chain of eq. (4.5), it can be recast as a sum of finitely many mirror processes (involving at most three mirror magnons), so that it can be evaluated directly. It is of course somewhat disappointing that these considerations, much like the ones at order g^2 and g^0 does not stem only from the internal consistency of the hexagon formalism, but require input from field theory.

5 Conclusions and outlook

In this paper we have improved on the naïve bound for the 't Hooft-coupling scaling of a hexagon form factor with a set of N_1, N_2, N_3 mirror magnons. That would have been order g^p with

$$p_{\text{naïve}} = \sum_{i=1}^{3} N_i \ell_i + (N_1 - N_2)^2 + N_3^2 - 2N_3(N_1 + N_2)\,, \tag{5.1}$$

which is unbounded from below as N_1, N_2 and N_3 grow—signalling an apparent breakdown of the weak-coupling perturbation theory for the hexagon form-factor program and flying in the face of established perturbative results such as those of refs. [9–11, 23]. We have shown that such naïve bound can be improved and is non-decreasing as N_1, N_2 and N_3 grow. Similar considerations apply in the presence of physical magnons.

However, even our improved formula allows for infinite "chains" of mirror particles at finite order in g^p. They appear only when two out of three bridge lengths ℓ_i vanish on a given hexagon. In the case of four-point functions, which we investigated at some length in section 4, this is what happens for tessellations built from *disconnected* tree-level graphs. While we could not find an argument to argue these chains away within the hexagon formalism, we have observed that in practice (taking into account field theory considerations) we do not need to compute such an infinite sum of terms; we can instead trade them for a finite sum of mirror-magnon contributions, at least up two loops in field theory—order g^4. It is not hard to believe that such infinite chains of magnons might simplify drastically: viewing the resulting sum-integrals as Mellin representations [10] one might *e.g.* expect that a chain of gluings over zero-width edges can be simplified as in Barnes' lemma.[7] Still it would be very interesting to understand from first principles whether such infinite chains of magnons should be disregarded and why.

Having a systematic understanding of the dynamics of mirror magnons is an important first step towards the summation of finite-size corrections to obtain a truly non-perturbative framework, perhaps along the lines of the mirror thermodynamic Bethe ansatz formalism for two-point functions. It is not obvious what is the best context to tackle this important and challenging problem. While the hexagon formalism is established only for

[6] We have checked this explicitly for all possible correlators of half-BPS operators when any operator has length from 2 to 7.

[7] B.E. thanks Benjamin Basso for a discussion on related matters.

AdS_5/CFT_4, where the integrability machinery is best developed, it is interesting to note that in integrable AdS_3/CFT_2 [34] there exist models where wrapping effects drastically simplify [35, 36]—in fact, they *vanish* for two-point functions—and where closed formulae exist for some correlation functions owing to worldsheet (Wess-Zumino-Witten) techniques. This might also be an excellent arena to test the hexagon program.

Let us also remark that the same reasoning that allowed us to circumvent infinite sums of mirror magnons (as explained in section 4) also leads us to a number of interesting observations which would greatly simplify the computation of the four-BPS correlator at order g^4. For instance, a rather problematic class of diagrams is the one which we can obtain from the disconnected ones of figure 4 by setting *e.g.* $\ell_{13} = 1$; we call these "sausage" graphs. There, infinite chains of mirror magnons do not appear but we find a large number of possible processes: at order g^2 we should consider up to *four* mirror magnons, while at order g^4 we should consider up to *eight* mirror magnons. Such a proliferation is worrying, as it makes the hexagon formalism very cumbersome. On the other hand, using the criteria 1.–5. of the section above, we can see that there are numerous cancellations, which happen graph-by-graph for processes involving different numbers of mirror magnons. In particular, processes involving four magnons are suppressed and only appear at order g^4, and processes involving five or more magnons only appear at order g^6. It is interesting to observe that this cancellation is also compatible with a further field-theory inspired constraint, that is the *maximum transcendentality* of a correlator increases with the order of g^2. Technically, this order appears in the hexagon formalism from the highest-pole order in the integrand of mirror processes. This pole comes[8] from the mirror measure and bridge-length contribution. On these grounds, we would expect that mirror integrals related to edges with length ℓ only contribute at order $g^{2\ell+2}$ or higher, as it is indeed the case for sausage graphs. In fact, this principle may be taken as an additional constraint in future hexagon-form-factor computations.

Acknowledgements

BE is supported by DFG "eigene Stelle" Ed 78/4-3. MdL was supported by SFI and the Royal Society for funding under grant UF160578. D. le Plat acknowledges support by the Stiftung der Deutschen Wirtschaft. AS's work is partially supported by the NCCR SwissMAP, funded by the Swiss National Science Foundation; he also acknowledges support by the ETH "Career Seed Grant" no. 0-20313-17.

A Algorithm for triple mirror scattering

In this section we give an alternative derivation of the number of triple scattering events $T(N_1, N_2, N_3)$ discussed in section 3. This derivation is based on an algorithmic derivation of the scattering process that maximize the number of triangles. In order to introduce the notation and explain the idea, we first consider a simple example with $(N_1, N_2, N_3) = (3, 3, 3)$. In what follows, we will denote the configuration (N_1, N_2, N_3) by

$$\underbrace{1\cdots1}_{N_1}\underbrace{2\cdots2}_{N_2}\underbrace{3\cdots3}_{N_3} \equiv (1)^{N_1}(2)^{N_2}(3)^{N_3} \tag{A.1}$$

[8] This can be seen most readily by rewriting the integrand by taking partial fractions, like in refs. [20, 21], and observing that partial fractioning preserves the order of the leading pole.

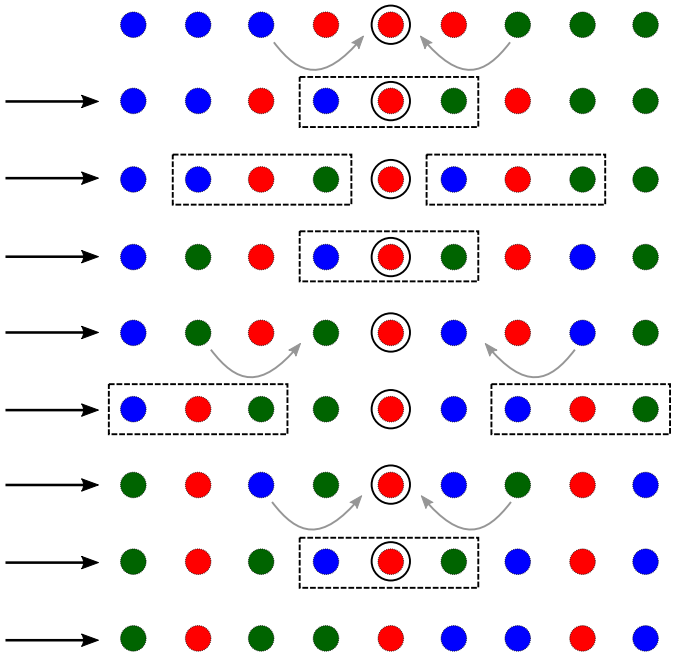

Figure 5. Diagrammatic representation for the scattering processes. The blue, red and green dots stand for particles 1 ,2 and 3 respectively. The circled red dot denotes the seed particle *2* and the dashed box represent the triple scattering process [1 2 3]. We see 7 triple scattering processes in the diagram.

We expect to have $T(3,3,3) = 7$ from the previous section. Here we demonstrate how this can be realized. We start with the configuration

$$1\,1\,1\,2\,\mathit{2}\,2\,3\,3\,3\,. \tag{A.2}$$

According to the hexagon form factor prescription, we move the 1 's to the right and 3 's to the left through scattering. The process is as follows

$$\begin{aligned} &1\,1\,1\,2\,\mathit{2}\,2\,3\,3\,3 \longrightarrow 1\,1\,2\,[1\,\mathit{2}\,3]\,2\,3\,3 \longrightarrow 1\,[1\,2\,3]\,\mathit{2}\,[1\,2\,3]\,3 \\ \longrightarrow\, &1\,3\,2\,[1\,\mathit{2}\,3]\,2\,1\,3 \longrightarrow 1\,3\,2\,3\,\mathit{2}\,1\,2\,1\,3 \longrightarrow [1\,2\,3]\,3\,\mathit{2}\,1\,[1\,2\,3] \\ \longrightarrow\, &3\,2\,1\,3\,\mathit{2}\,1\,3\,2\,1 \longrightarrow 3\,2\,3\,[1\,\mathit{2}\,3]\,1\,2\,1 \longrightarrow 3\,2\,3\,3\,\mathit{2}\,1\,1\,2\,1 \end{aligned} \tag{A.3}$$

The rest scattering process do not involve triple scattering process that we are looking for so we stop here. In the above, the particle in the middle is denoted by italic font *2*. This particle is special for our algorithm and is called the *seed particle*. The triple scattering process, which corresponds to the triangle in the previous section is denoted by

$$\cdots [1\,2\,3]\cdots \longrightarrow \cdots 3\,2\,1\,\cdots \tag{A.4}$$

The process described in (A.3) can be represented diagrammatically as in figure 5. Now we give the general proof. As before, we need to consider several cases while performing the counting. We split the scattering process into two parts. The first part is universal for all the cases. The second part depend on the cases we consider.

A.1 Universal move

We start with the following configuration with the seed particle

$$1^{N_1}2^{N_2}3^{N_3} = 1^{N_1}2^{S}\mathcal{2}2^{N_2-S-1}3^{N_3}, \tag{A.5}$$

where

$$S = \left[\frac{N_1+N_2-N_3}{2}\right]. \tag{A.6}$$

We move the particles 1 /3 towards the seed particle from the left/right. The first step is

$$\begin{aligned} 1^{N_1}2^{S}\mathcal{2}2^{N_2-S-1}3^{N_3} &\longrightarrow 1^{N_1-1}2^{S}[1\,\mathcal{2}\,3]2^{N_2-S-1}3^{N_3-1} \\ &= 1^{N_1-1}2^{S}3\,\mathcal{2}\,1\,2^{N_2-S-1}3^{N_3-1} \\ &= 1^{N_1-1}2^{S-1}(2\,3)\mathcal{2}(1\,2)2^{N_2-S-2}3^{N_3-1}. \end{aligned} \tag{A.7}$$

For the l-th step, we perform the move

$$\begin{aligned} & 1^{N_1-l+1}2^{S-l+1}(2\,3)^{l-1}\mathcal{2}(1\,2)^{l-1}2^{N_2-S-l}3^{N_3-l+1} \\ \longrightarrow\ & 1^{N_1-l}2^{S-l+1}1\,(2\,3)^{l-1}\mathcal{2}(1\,2)^{l-1}3\,2^{N_2-S-l}3^{N_3-l} \\ \longrightarrow\ & 1^{N_1-l}2^{S-l+1}(3\,2)^{l-1}[1\,\mathcal{2}\,3](2\,1)^{l-1}2^{N_2-S-l}3^{N_3-l} \\ \longrightarrow\ & 1^{N_1-l}2^{S-l+1}(3\,2)^{l-1}3\,\mathcal{2}\,1\,(2\,1)^{l-1}2^{N_2-S-l}3^{N_3-l} \\ =\ & 1^{N_1-l}2^{S-l}(2\,3)^{l}\mathcal{2}(1\,2)^{l}2^{N_2-S-l-1}3^{N_3-l}. \end{aligned} \tag{A.8}$$

The number of triple scattering processes involved in the l-th step is $2l-1$. We can perform this move until one of the exponents N_1-l, $S-1$, $N_2-S-l-1$ and N_3-l becomes zero. Therefore we need to distinguish between different cases. First we say without loss of generality $N_2 \geq N_3$ and $N_2 \geq N_1$. We can ever obtain this by cyclicity. We consider the case that $N_1 \leq N_3$. The case with $N_1 > N_3$ can be considered in a similar way. In the next subsection, we consider different cases.

A.2 The case $S > N_1$ and $N_3 \geq N_1$

For this case, we have $N_2 \geq N_1 + N_3$. The universal move stops because $N_1 - l$ becomes zero and we end up with the following configuration

$$2^{S-N_1}(2\,3)^{N_1}\mathcal{2}(1\,2)^{N_1}2^{N_2-S-N_1-1}3^{N_3-N_1}. \tag{A.9}$$

For the rest consideration, the seed particle is not important anymore, so we treat it as the rest 2 particles. We perform the following move

$$\begin{aligned} & 2^{S-N_1}(2\,3)^{N_1}2\,(1\,2)^{N_1}2^{N_2-S-N_1-1}3^{N_3-N_1} \\ \longrightarrow\ & 2^{S-N_1}(2\,3)^{N_1}2\,[(1\,2)^{N_1}3\,]2^{N_2-S-N_1-1}3^{N_3-N_1-1} \\ \longrightarrow\ & 2^{S-N_1}(2\,3)^{N_1}2\,3\,(2\,1)^{N_1}2^{N_2-S-N_1-1}3^{N_3-N_1-1} \\ =\ & 2^{S-N_1}(2\,3)^{N_1+1}2\,(1\,2)^{N_1}2^{N_2-S-N_1-2}3^{N_3-N_1-1}. \end{aligned} \tag{A.10}$$

This kind of move can be performed N_3-N_1 times. Each move involves N_1 triple scattering process. Finally we end up with the following configuration

$$2^{S-N_1}(2\,3\,)^{N_3}2\,(1\,2\,)^{N_1}2^{N_2-S-N_3-1}. \tag{A.11}$$

Taking the sum of the two steps, we find the number of triangle scattering processes

$$T(N_1, N_2, N_3) = \sum_{l=1}^{N_1}(2l-1) + N_1(N_3 - N_1) = N_1 N_3, \tag{A.12}$$

which matches what we obtained in the section 3 for cases I and III.

A.3 The case $S \leq N_1$ and $N_3 > N_1$

For this case, the universal move stops because $S - l$ becomes zero and we end up with the following configuration

$$1^{\,N_1-S}(2\,3)^S 2\,(1\,2)^S 2^{\,N_2-2S-1} 3^{\,N_3-S}. \tag{A.13}$$

To obtain the rest of the triple scattering processes, we first perform the following move

$$\begin{aligned} & 1^{\,N_1-S}(2\,3)^S 2\,(1\,2)^S 2^{\,N_2-2S-1} 3^{\,N_3-S} \\ =\, & 1^{\,N_1-S-1}[1\,(2\,3)^S]2\,(1\,2)^S 2^{\,N_2-2S-1} 3^{\,N_3-S} \\ \longrightarrow\, & 1^{\,N_1-S-1}(3\,2)^S 1\,2\,(1\,2)^S 2^{\,N_2-2S-1} 3^{\,N_3-S} \\ =\, & 1^{\,N_1-S-1} 3\,(2\,3)^{S-1} 2\,(1\,2)^{S+1} 2^{\,N_2-2S-1} 3^{\,N_3-S}. \end{aligned} \tag{A.14}$$

This move involves S triple scattering processes. Then we perform the following recursive move. At step-l, we have

$$\begin{aligned} & 1^{\,N_1-S-l} 3^{\,l}(2\,3)^{S-1} 2\,(1\,2)^{S+l} 2^{\,N_2-2S-l} 3^{\,N_3-S-l+1} \\ \longrightarrow\, & 1^{\,N_1-S-l-1} 3^{\,l}[1\,(2\,3)^{S-1}]2\,[(1\,2)^{S+l} 3]2^{\,N_2-2S-l} 3^{\,N_3-S-l} \\ \longrightarrow\, & 1^{\,N_1-S-l-1} 3^{\,l}(3\,2)^{S-1}[1\,2\,3](1\,2)^{S+l} 2^{\,N_2-2S-l} 3^{\,N_3-S-l} \\ \longrightarrow\, & 1^{\,N_1-S-l-1} 3^{\,l}(3\,2)^{S-1} 3\,2\,1\,(2\,1)^{S+l} 2^{\,N_2-2S-l} 3^{\,N_3-S-l} \\ =\, & 1^{\,N_1-S-l-1} 3^{\,l+1}(2\,3)^{S-1} 2\,(1\,2)^{S+l+1} 2^{\,N_2-2S-l-1} 3^{\,N_3-S-l}. \end{aligned} \tag{A.15}$$

Here again we have two different cases where these processes can end, depending on whether $N_1 - S - 1$ or $N_2 - 2S - 1$ is larger. We consider cases one by one.

1. The case $N_2 - N_1 \geq S$, the process ends because $N_1 - S - l - 1$ becomes zero. We end up with the following configuration

$$3^{\,N_1-S}(2\,3)^{S-1} 2\,(1\,2)^{N_1} 2^{\,N_2-N_1-S} 3^{\,N_3-N_1+1}. \tag{A.16}$$

   To proceed, we perform the following recursive move. For step-l, we have

$$\begin{aligned} & 3^{\,N_1-S}(2\,3)^{S+l-2} 2\,(1\,2)^{N_1} 2^{\,N_2-N_1-S-l+1} 3^{\,N_3-N_1-l+2} \\ \longrightarrow\, & 3^{\,N_1-S}(2\,3)^{S+l-2} 2\,[(1\,2)^{N_1} 3]2^{\,N_2-N_1-S-l+1} 3^{\,N_3-N_1-l+1} \\ \longrightarrow\, & 3^{\,N_1-S}(2\,3)^{S+l-2} 2\,3\,(2\,1)^{N_1} 2^{\,N_2-N_1-S-l+1} 3^{\,N_3-N_1-l+1} \\ =\, & 3^{\,N_1-S}(2\,3)^{S+l-1} 2\,(1\,2)^{N_1} 2^{\,N_2-N_1-S-l} 3^{\,N_3-N_1-l+1}. \end{aligned} \tag{A.17}$$

   Each step involves N_1 and will stop for $l = N_2 - N_1 - S$. So the total number of triple scattering processes is $N_1(N_2 - N_1 - S)$. We end up with the following configuration

$$3^{\,N_1-S}(2\,3)^{N_2-N_1-1} 2\,(1\,2)^{N_1} 3^{\,N_3-N_2+S+1}. \tag{A.18}$$

As the last step, we perform the following recursive move, for the l-th step

$$\begin{aligned} &3^{N_1-S}(2\,3)^{N_2-N_1+l-1}2\,(1\,2)^{N_1-l}1\,l\,3^{N_3-N_2+S-l+1} \\ \longrightarrow\ &3^{N_1-S}(2\,3)^{N_2-N_1+l-1}2\,[(1\,2)^{N_1-l}3]1\,l\,3^{N_3-N_2+S-l} \\ \longrightarrow\ &3^{N_1-S}(2\,3)^{N_2-N_1+l-1}2\,3\,(2\,1)^{N_1-l}1\,l\,3^{N_3-N_2+S-l} \\ =\ &3^{N_1-S}(2\,3)^{N_2-N_1+l}2\,(1\,2)^{N_1-l-1}1\,l+1\,3^{N_3-N_2+S-l}. \end{aligned} \tag{A.19}$$

This stops at $l = N_3 - N_2 + S$ and end up with the following configuration

$$3^{N_1-S}(2\,3)^{N_3-N_1+S}2\,(1\,2)^{N_1+N_2-N_3-S-1}1^{N_3-N_2+S+1}. \tag{A.20}$$

We can not produce further triple scattering processes. Summing up the number of triple scattering processes, we obtain

$$\begin{aligned} T(N_1,N_2,N_3) &= \sum_{l=1}^{S}(2l-1) + S + \sum_{l=1}^{N_1-S-1}(2S+l) + N_1(N_2-N_1-S) \\ &\quad + N_1 + \sum_{l=1}^{N_3-N_2+S}(N_1-l) \\ &= -\frac{1}{4}\left(N_1^2+N_2^2+N_3^2-2N_1N_2-2N_1N_3-2N_2N_3-c\right), \end{aligned} \tag{A.21}$$

where $c = \mathrm{mod}[N_1+N_2+N_3, 2]$. Using the result, we find that the order g^p is given by

$$p = \sum_{i=1}^{3}\ell_i N_i + \frac{1+(-1)^{\sum_i N_i}}{2}. \tag{A.22}$$

2. The case $N_2 - N_1 < S$, the process ends because $N_2 - 2S - 1$ becomes zero. We end up with the following configuration

$$1^{N_1-N_2+S}3^{N_2-2S}(2\,3)^{S-1}2\,(1\,2)^{N_2-S}3^{N_3-N_2+S+1}. \tag{A.23}$$

We now perform the following recursive move at l-th step. Here we get $N_2 - S - l + 1$ triples.

$$\begin{aligned} &1^{N_1-N_2+S}3^{N_2-2S}(2\,3)^{S+l-2}2\,(1\,2)^{N_2-S-l+1}1^{l-1}3^{N_3-N_2+S+2-l} \\ \longrightarrow &1^{N_1-N_2+S}3^{N_2-2S}(2\,3)^{S+l-1}2\,(1\,2)^{N_2-S-l}1\,l\,3^{N_3-N_2+S+1-l}. \end{aligned} \tag{A.24}$$

This procedure stops when $N_3 - N_2 + S + 1 - l$ goes to zero. We get the following configuration:

$$1^{N_1-N_2+S}3^{N_2-2S}(2\,3)^{N_3-N_2+2S}2\,(1\,2)^{2N_2-2S-N_3-1}1^{N_3-N_2+S+1}. \tag{A.25}$$

We now move all the 1 from the left across all $(2\,3)$. At l-th step again we get the following move:

$$\begin{aligned} &1^{N_1-N_2+S-l+1}3^{N_2-2S+l-1}(2\,3)^{N_3-N_2+2S-l+1}2\,(1\,2)^{2N_2-2S-N_3-l}1^{N_3-N_2+S+1} \\ \longrightarrow &1^{N_1-N_2+S-l}3^{N_2-2S+l}(2\,3)^{N_3-N_2+2S-l}2\,(1\,2)^{2N_2-2S-N_3-l-1}1^{N_3-N_2+S+1}. \end{aligned} \tag{A.26}$$

By doing this step we get $N_3-N_2+2S-l+1$ new triples. This is possible until N_1-N_2+S-l goes to zero. Then we end up with:

$$3^{\,N_1-S}(2\,3\,)^{N_3-N_1+S}2\,(1\,2\,)^{N_2-S-N_3+N_1-1}1^{\,N_3-N_2+S+1}. \tag{A.27}$$

Here we cannot produce any more triples again. Counting all triples we get the following.

$$\begin{aligned} T(N_1,N_2,N_3) = &\sum_{l=1}^{S}(2l-1)+S+\sum_{l=1}^{N_2-2S-1}(2S+l)+\sum_{l=1}^{N_3-N_2+S+1}(N_2-S-l+1)\\ &+\sum_{l=1}^{N_1-N_2+S}(N_3-N_2+2S-l+1). \end{aligned} \tag{A.28}$$

Simplifying this expression we obtain a result for p similar to (A.22).

A.4 The case $N_3 = N_1$ and $S \leq N_3$

In this case, we have again $N_2 \leq N_1 + N_3 = 2N_3$. With this constraints we get $S = \left[\frac{N_2}{2}\right]$. The universal move stops because $N_2-S-1-l$ becomes zero. We now consider to different cases.

1. We consider first that N_2 is even, then $S = \frac{N_2}{2}$. So we end up with the following configuration:

$$1^{\,N_3-S+1}2\,(2\,3\,)^{S-1}2\,(1\,2\,)^{S-1}3^{\,N_3-S+1}. \tag{A.29}$$

We now perform the following move and get $S-1$ triples.

$$\begin{aligned} &1^{\,N_3-S+1}2\,(2\,3\,)^{S-1}2\,(1\,2\,)^{S-1}3^{\,N_3-S+1}\\ \longrightarrow &1^{\,N_3-S}(2\,3\,)^{S-1}2\,(1\,2\,)^{S}3^{\,N_3-S+1}. \end{aligned} \tag{A.30}$$

Now we move recursively a 1 from the left and a 3 from the right simultaneously to the middle as shown in (A.31). Here we get at the l-th step $2S$ new triples.

$$\begin{aligned} &1^{\,N_3-S-l+1}3^{\,l-1}(2\,3\,)^{S-1}2\,(1\,2\,)^{S}1^{\,l-1}3^{\,N_3-S+2-l}\\ =&1^{\,N_3-S-l}3^{\,l-1}[1\,(2\,3\,)^{S-1}]2\,[(1\,2\,)^{S}3\,]1^{\,l-1}3^{\,N_3-S+1-l}\\ \longrightarrow&1^{\,N_3-S-l}3^{\,l-1}(3\,2\,)^{S-1}[1\,2\,3\,](2\,1\,)^{S}1^{\,l-1}3^{\,N_3-S+1-l}\\ \longrightarrow&1^{\,N_3-S-l}3^{\,l}(2\,3\,)^{S-1}2\,(1\,2\,)^{S}1^{\,l}3^{\,N_3-S+1-l}. \end{aligned} \tag{A.31}$$

This recursion ends if $N3-S-l$ becomes zero and we end up with the following:

$$3^{\,N_3-S}(2\,3\,)^{S-1}2\,(1\,2\,)^{S}1^{\,N3-S}3\,. \tag{A.32}$$

By moving the 3 on the right through the $(1\,2\,)$'s we get S triples and cannot perform other triple moves then. All in all the sum of the triples is

$$\begin{aligned} T(N_3,N_2,N_3) &= \sum_{l=1}^{S-1}+S-1+\sum_{l=1}^{N_3-S}(2S)+S\\ &= -\frac{N_2^2}{4}+N_2N_3. \end{aligned} \tag{A.33}$$

This is the same like in (A.21) with $N_1 = N_3$ and N_2 even. So we end up with formula (A.22) for p.

2. Now we consider that N_2 is odd, then $S = \frac{N2}{2} - \frac{1}{2}$. From universal move we end up with:

$$1^{N_3-S}2\,(2\,3\,)^S 2\,(1\,2\,)^S 3^{N_3-S}. \tag{A.34}$$

Now we move recursively a 1 from the left and a 3 from the right to the middle as shown below. At l-th step we get $2S+1$ triples.

$$\begin{aligned} &1^{N_3-S-l+1}3^{l-1}(2\,3\,)^S 2\,(1\,2\,)^S 1^{l-1}3^{N_3-S-l+1} \\ =&1^{N_3-S-l}3^{l-1}[1\,(2\,3\,)^S]2\,[(1\,2\,)^S 3\,]1^{l-1}3^{N_3-S-l} \\ \longrightarrow&1^{N_3-S-l}3^{l-1}(3\,2\,)^S[1\,2\,3\,](2\,1\,)^S 1^{l-1}3^{N_3-S-l} \\ \longrightarrow&1^{N_3-S-l}3^{l}(2\,3\,)^S 2\,(1\,2\,)^S 1^{l}3^{N_3-S-l}. \end{aligned} \tag{A.35}$$

This procedure ends if $N_3 - S - l$ becomes zero. After that it is not possible to do another triple move. All in all the sum of the triples is

$$T(N_1, N_2, N_3) = \sum_{l=1}^{S}(2l-1) + \sum_{l=1}^{N3-S}(2S+1) \tag{A.36}$$

$$= -\frac{1}{4}\left(N_2^2 - 4N_2N_3 - 1\right). \tag{A.37}$$

Which is also the same like in (A.21) with $N_1 = N_3$ and N_2 odd. So we end up with formula (A.22) for p.

References

[1] J. M. Maldacena, *The Large N limit of superconformal field theories and supergravity*, *Int. J. Theor. Phys.* **38** (1999) 1113 [hep-th/9711200].

[2] E. Witten, *Anti-de Sitter space and holography*, *Adv. Theor. Math. Phys.* **2** (1998) 253 [hep-th/9802150].

[3] S. S. Gubser, I. R. Klebanov and A. M. Polyakov, *Gauge theory correlators from non-critical string theory*, *Phys. Lett.* **B428** (1998) 105 [hep-th/9802109].

[4] G. 't Hooft, *A planar diagram theory for strong interactions*, *Nucl. Phys.* **B72** (1974) 461.

[5] J. A. Minahan and K. Zarembo, *The Bethe-ansatz for $\mathcal{N} = 4$ super Yang-Mills*, *JHEP* **0303** (2003) 013 [hep-th/0212208].

[6] G. Arutyunov and S. Frolov, *Foundations of the $AdS5 \times S^5$ superstring. part I*, *J. Phys. A* **A42** (2009) 254003 [0901.4937].

[7] N. Beisert et al., *Review of AdS/CFT integrability: An overview*, *Lett. Math. Phys.* **99** (2012) 3 [1012.3982].

[8] B. Basso, S. Komatsu and P. Vieira, *Structure constants and integrable bootstrap in planar $\mathcal{N} = 4$ SYM theory*, 1505.06745.

[9] B. Eden and A. Sfondrini, *Tessellating cushions: four-point functions in $\mathcal{N} = 4$ SYM*, *JHEP* **10** (2017) 098 [1611.05436].

[10] T. Fleury and S. Komatsu, *Hexagonalization of Correlation Functions*, *JHEP* **01** (2017) 130 [1611.05577].

[11] B. Eden, Y. Jiang, D. le Plat and A. Sfondrini, *Colour-dressed hexagon tessellations for correlation functions and non-planar corrections*, *JHEP* **02** (2018) 170 [1710.10212].

[12] T. Bargheer, J. Caetano, T. Fleury, S. Komatsu and P. Vieira, *Handling Handles I: Nonplanar Integrability*, 1711.05326.

[13] W. Carlson, R. de Mello Koch and H. Lin, *Nonplanar Integrability*, *JHEP* **03** (2011) 105 [1101.5404].

[14] R. de Mello Koch, M. Kim and H. J. R. Zyl, *Integrable Subsectors from Holography*, *JHEP* **05** (2018) 198 [1802.01367].

[15] C. Kristjansen, *Review of AdS/CFT integrability, Chapter IV.1: Aspects of non-planarity*, *Lett. Math. Phys.* **99** (2010) 349 [1012.3997].

[16] N. Beisert and M. Staudacher, *Long-range* PSU$(2,2|4)$ *Bethe ansaetze for gauge theory and strings*, *Nucl. Phys.* **B727** (2005) 1 [hep-th/0504190].

[17] J. Ambjørn, R. A. Janik and C. Kristjansen, *Wrapping interactions and a new source of corrections to the spin-chain/string duality*, *Nucl. Phys.* **B736** (2006) 288 [hep-th/0510171].

[18] M. Lüscher, *Volume dependence of the energy spectrum in massive quantum field theories. 1. Stable particle states*, *Commun. Math. Phys.* **104** (1986) 177.

[19] M. Lüscher, *Volume dependence of the energy spectrum in massive quantum field theories. 2. Scattering states*, *Commun. Math. Phys.* **105** (1986) 153.

[20] B. Eden and A. Sfondrini, *Three-point functions in $\mathcal{N} = 4$ SYM: the hexagon proposal at three loops*, *JHEP* **02** (2016) 165 [1510.01242].

[21] B. Basso, V. Goncalves, S. Komatsu and P. Vieira, *Gluing Hexagons at Three Loops*, *Nucl. Phys.* **B907** (2016) 695 [1510.01683].

[22] B. Basso, V. Goncalves and S. Komatsu, *Structure constants at wrapping order*, *JHEP* **05** (2017) 124 [1702.02154].

[23] T. Fleury and S. Komatsu, *Hexagonalization of Correlation Functions II: Two-Particle Contributions*, *JHEP* **02** (2018) 177 [1711.05327].

[24] N. Beisert, *The* $SU(2|2)$ *dynamic S-matrix*, *Adv. Theor. Math. Phys.* **12** (2008) 945 [hep-th/0511082].

[25] G. Arutyunov, M. de Leeuw and A. Torrielli, *The bound state S-matrix for AdS5 $\times$ S^5 superstring*, *Nucl. Phys.* **B819** (2009) 319 [0902.0183].

[26] N. Beisert, B. Eden and M. Staudacher, *Transcendentality and crossing*, *J. Stat. Mech.* **0701** (2007) P01021 [hep-th/0610251].

[27] G. Arutyunov, S. Frolov and M. Zamaklar, *The Zamolodchikov-Faddeev algebra for AdS(5) x S**5 superstring*, *JHEP* **04** (2007) 002 [hep-th/0612229].

[28] G. Arutyunov and S. Frolov, *The dressing factor and crossing equations*, *J. Phys.* **A42** (2009) 425401 [0904.4575].

[29] J. M. Drummond, J. Henn, V. A. Smirnov and E. Sokatchev, *Magic identities for conformal four-point integrals*, *JHEP* **01** (2007) 064 [hep-th/0607160].

[30] E. D'Hoker, D. Z. Freedman, S. D. Mathur, A. Matusis and L. Rastelli, *Extremal correlators in the AdS / CFT correspondence*, hep-th/9908160.

[31] M. Bianchi and S. Kovacs, *Nonrenormalization of extremal correlators in N=4 SYM theory*, *Phys. Lett.* **B468** (1999) 102 [hep-th/9910016].

[32] B. Eden, P. S. Howe, C. Schubert, E. Sokatchev and P. C. West, *Extremal correlators in four-dimensional SCFT*, *Phys. Lett.* **B472** (2000) 323 [hep-th/9910150].

[33] D. Chicherin, J. Drummond, P. Heslop and E. Sokatchev, *All three-loop four-point correlators of half-BPS operators in planar $\mathcal{N} = 4$ SYM*, *JHEP* **08** (2016) 053 [1512.02926].

[34] A. Sfondrini, *Towards integrability for AdS3/CFT$_2$*, *J. Phys.* **A48** (2015) 023001 [1406.2971].

[35] M. Baggio and A. Sfondrini, *Strings on NS-NS Backgrounds as Integrable Deformations*, 1804.01998.

[36] A. Dei and A. Sfondrini, *Integrable spin chain for stringy Wess-Zumino-Witten models*, 1806.00422.